Quantum Electronics **52** (1) 87 – 93 (2022) © 2022 Kvantovaya Elektronika and IOP Publishing Limited

FIBRE-OPTIC SYSTEMS

https://doi.org/10.1070/QEL17970

Effect of anisotropy of a single-mode fibre on lightning-induced rotation of polarisation of a light signal in an optical ground wire

D.V. Gorbatov, V.A. Konyshev, T.O. Lukinykh, O.E. Nanii, A.G. Novikov, V.N. Treshchikov, R.R. Ubaydullaev

Abstract. **A numerical model is constructed for calculating lightning-induced rapid changes in the polarisation state of a light signal at the output of a fibre-optic communication line with an optical ground wire. It is shown that taking into account anisotropy of real optical fibres has a noticeable effect on the shape of the polarisation rotation speed time profile. It is found that the maximum rate of change in the polarisation state and its temporal profile depend on the location of the lightning strike in the fibre span, the magnitude of fibre anisotropy and the direction of propagation of a light wave.**

Keywords: *FOCL, OPGW, lightning strike, high-voltage power line, optical ground wire, Faraday effect, standard single-mode fibre, optical fibre anisotropy, coherent transmission line, polarisation rotation speed, polarisation state, bit error rate.*

1. Introduction

The use of optical ground wires (OPGWs) is a cost-effective technical solution, since it allows one to simultaneously combine the functions of grounding, which shields power lines from lightning strikes, and telecommunication, which is used for data transmission over optical fibres.

However, a direct lightning strike in an OPGW, as it turned out, can cause short-term interruptions in communication when using modern coherent high-speed information transmission systems. Today, the physical mechanism of this phenomenon is generally clear: a lightning strike forms a strong longitudinal magnetic field in fibre, a change in which, in turn, leads to the rotation of the polarisation state of the optical signal due to the Faraday effect and to the appearance of errors on the receiving side [1, 2]. Modern high-speed coherent transmission systems with multilevel modulation formats and polarisation-division multiplexing are most sensitive to lightning strikes.

Thus, practical needs in protecting fibre-optic communication lines (FOCLs) with OPGWs from communication interruptions caused by lightning strikes into an optical ground wire made it necessary to study the Faraday effect in optical telecommunication fibres and to calculate the peak values and the shape of the time dependence of the rate of change in the polarisation state of light signals at the OPGW output. In addition, the measured characteristics of lightning-induced changes in the polarisation state of light transmitted through a FOCL with an OPGW can be used to find the location of a lightning strike and calculate the peak current value, if the connection between the lightning parameters and the polarisation dynamics is established.

It is shown in [3] that for lightnings with steep fronts (∼1 μs), it is necessary to take into account the finite time of the establishment of the electric field in the ground wire and the finite time of propagation of the light wave in optical fibre. At the same time, in calculating the rate of change in the polarisation state due to the Faraday effect in [3], optical fibre was considered isotropic. An analysis of the influence of birefringence on the value of the polarisation rotation angle by a magnetic field was performed in [4], where the statistically averaged dependences of the change in the polarisation rotation angle on the applied magnetic field were studied experimentally and using numerical simulation. However, this work did not consider the dynamic effects associated with the fast rotation of the polarisation state, and the fibre length (50 km) was two orders of magnitude longer than the typical length of a span (300 – 400 m) between pylons of a FOCL with OPGWs.

In this work, for the first time, using numerical simulation, we analyse the effect of the telecommunication fibre anisotropy on the time dependences of the rate of change in the polarisation state under the action of a magnetic field produced by a direct lightning strike into an OPGW.

2. Methods of Jones matrices and Mueller matrices

We will use the Jones matrix method for quantitative description of the change in the polarisation state of optical radiation propagating in fibre. In this method, optical elements through which light passes, and primarily fibre, can be functionally described by complex matrices 2×2 that form a special unitary group SU(2), i.e. Jones matrices. The Jones matrix J of an optical element consisting of two sequential optical ele-

D.V. Gorbatov, V.A. Konyshev, T.O. Lukinykh, A.G. Novikov, R.R. Ubaydullaev T8 LLC, Krasnobogatyrskaya ul. 44/1, 107076 Moscow, Russia; e-mail: konyshev@t8.ru;
O.E. Nanii T8 LLC, Krasnobogatyrskaya ul. 44/1, 107076 Moscow, Russia; Faculty of Physics, Lomonosov Moscow State University, Leninskie Gory, 119991 Moscow, Russia;
e-mail: naniy@t8.ru;
V.N. Treshchikov T8 LLC, Krasnobogatyrskaya ul. 44/1107076 Moscow, Russia; Kotelnikov Institute of Radioengineering and Electronics (Fryazino Branch), Russian Academy of Sciences, pl. Akad. Vvedenskogo 1, 141190 Fryazino, Moscow region, Russia

Received 18 October 2021; revision received 10 November 2021
Kvantovaya Elektronika **52** (1) 87 – 93 (2022)
Translated by I.A. Ulitkin

ments is equal to the product of Jones matrices J_1 and J_2 of these elements, taken in reverse order: $J = J_2 J_1$. In this case, the polarisation states are described by Jones vectors – two-component vectors of unit length in the general case with complex components $|s\rangle = (E_x, E_y)^{\mathrm{T}}$, where $|E_x|^2 + |E_y|^2 = 1$. The relationship of polarisation states at the input, $|s\rangle$, and at the output, $|t\rangle$, of the optical element with the matrix J is as follows: the Jones vector at the output of the optical element is equal to the product of the Jones matrix of the optical element by the Jones vector at the input to the optical element: $|t\rangle = J|s\rangle$.

Along with the Jones formalism, we will also use the Mueller matrix method. We will not be interested in the unpolarised component of optical radiation. In this case, the optical element matrices are 3×3 matrices with real elements forming a special orthogonal group SO(3). The polarisation states in this method are described by three-component vectors of unit length with real components – Stokes vectors $\hat{\boldsymbol{s}} = (s_1, s_2, s_3)^{\mathrm{T}}$, where $s_1^2 + s_2^2 + s_3^2 = 1$. As in the Jones matrix method, there is a matrix relationship of the polarisation states at the input and output of the optical element: the Stokes vector $\hat{\boldsymbol{t}}$ at the output of the optical element is equal to the product of the Mueller matrix M of the optical element by the Stokes vector $\hat{\boldsymbol{s}}$ at the input to the optical element: $\hat{\boldsymbol{t}} = M\hat{\boldsymbol{s}}$. The components of the Stokes vector are uniquely determined by the components of the Jones vector using the relations

$$s_1 = E_x^2 - E_y^2,$$
$$s_2 = E_x E_y^* + E_x^* E_y, \qquad (1)$$
$$s_3 = \mathrm{i}(E_x E_y^* - E_x^* E_y).$$

The presence of three components and the unit length of the Stokes vectors determine their geometric position – a sphere of unit radius, which is commonly called the Poincaré sphere. Although Stokes vectors, unlike Jones vectors, are physically observable, and this information is provided by an optical polarimeter, it is convenient to perform numerical simulation directly using the Jones matrix method, and only where there is a need for experimental verification, it makes sense to convert Jones vectors into Stokes vectors.

3. Quantitative characteristics of changes in the polarisation state

The fastest changes in the polarisation state are observed at short time intervals of a steep rise of the lightning current, the duration of which can be from one to tens of microseconds [2, 3]. At such short time intervals, changes in the random birefringence distribution profile along fibre can be neglected. In what follows, we will adhere to the notations adopted in [4].

3.1. Spherical angle and spherical polarisation rotation speed

The polarisation state of the output radiation is described by a point on the Poincaré unit sphere, the trajectory of which due to the change in the longitudinal magnetic field in time will be called the trajectory of the polarisation state. For a quantitative description of changes in the polarisation state, we define the spherical angle $\theta(t)$ as the length of the polarisation state trajectory. From this definition it follows that the angle $\theta(t)$ is a nondecreasing function of time, which can be expressed in terms of small increments of angles between successive Stokes vectors. Therefore, we divide the entire interval $[0, t]$ into the intervals $\Delta t = t_n - t_{n-1}$, where $n = 0, 1, \ldots, N$. Let some input polarisation state $\hat{\boldsymbol{s}}_{\mathrm{in}}$ be given and the polarisation states at the output $\hat{\boldsymbol{s}}_0, \hat{\boldsymbol{s}}_1, \ldots, \hat{\boldsymbol{s}}_N$ be known at times $t_0, t_1, \ldots, t_N$, then

$$\theta(t_n, \hat{\boldsymbol{s}}_{\mathrm{in}}) = \sum_{k=1}^{n} \Delta\theta(\hat{\boldsymbol{s}}_{k-1}, \hat{\boldsymbol{s}}_k), \quad n = 1, 2, \ldots, N, \qquad (2)$$

where $\Delta\theta(\hat{\boldsymbol{s}}_{k-1}, \hat{\boldsymbol{s}}_k)$ are the angles between successive Stokes vectors defined by their scalar product:

$$\Delta\theta(\hat{\boldsymbol{s}}_{k-1}, \hat{\boldsymbol{s}}_k) = \arccos(\hat{\boldsymbol{s}}_{k-1}, \hat{\boldsymbol{s}}_k)$$
$$= \arccos(s_{1\,k-1} s_{1\,k} + s_{2\,k-1} s_{2\,k} + s_{3\,k-1} s_{3\,k}). \qquad (3)$$

Let us define the spherical polarisation rotation speed Ω_{s} as the time derivative of the spherical angle:

$$\Omega_{\mathrm{s}}(t) = \frac{\mathrm{d}\theta}{\mathrm{d}t}. \qquad (4)$$

The spherical rotation speed, taking into account (2), is transformed to the form

$$\Omega_{\mathrm{s}}(t_n) = \frac{\Delta\theta(\hat{\boldsymbol{s}}_{n-1}, \hat{\boldsymbol{s}}_n)}{\Delta t}. \qquad (5)$$

In the particular case of an isotropic optical element and linearly polarised input radiation, in the physical space the Faraday effect manifests itself in the rotation of the polarisation plane of linearly polarised radiation by an angle Θ around its propagation axis z (at the output, the radiation remains linearly polarised). In the Stokes space, in this case, the point describing the polarisation state of radiation rotates around the s_3 axis in the $s_1 s_2$ plane by an angle θ. The relationship between the angles has the simplest form:

$$\theta = 2\Theta. \qquad (6)$$

Using the well-known expression for describing the Faraday effect in an isotropic medium for linearly polarised radiation, the relationship between the spherical angle and the magnetic field is expressed as [5]:

$$\theta = 2VBL, \qquad (7)$$

where V is the specific Verdet constant of the optical element (for a single-mode optical fibre at a radiation wavelength of 1550 nm, $V = 0.53$ rad T^{-1} m^{-1} [6]); B is the magnetic field; and L is the length of the optical element.

In the considered case of linearly polarised radiation at the input to an isotropic medium, an increase in the magnetic field makes the point describing the polarisation state move along a great circle of the Poincaré sphere in the $s_1 s_2$ plane, and the spherical angle of the polarisation state is related to the magnetic field by formula (7).

In the case of elliptical polarisation, a change in the magnetic field makes the point describing the polarisation state move around the s_3 axis along a circle with a radius less than unity. The spherical angle corresponding to this trajectory of the polarisation state, when the magnetic field changes from zero to B, will be less than the angle calculated by formula (7). The closer the input polarisation to the circular one, i.e., the closer the modulus of the projection of the polarisation state vector onto the s_3 axis to 1, the smaller the radius of the circle along which this vector moves, and the smaller the corresponding spherical angle.

The main advantage of using the spherical angle and the spherical polarisation rotation speed is a relatively simple experimental measurement using a polarimeter that sequentially measures the polarisation state. The main disadvantage of using a spherical angle is its dependence on the input polarisation state.

3.2. Plane angle and plane polarisation rotation speed

For an isotropic optical element, the Faraday effect manifests itself in the rotation of the point describing the output state of polarisation on the Poincaré sphere, along a certain circle, the radius of which is not necessarily equal to unity. We define the plane angle $\varphi(t)$ as the angle through which the radius vector drawn from the centre of this circle to a point moving along the circle, describing the polarisation state at the output of the optical element, rotates.

The plane angle, in contrast to the spherical angle, is an invariant of the input polarisation. It can be reconstructed on the basis of experimental data even if there are static optical elements with unknown polarisation state rotation matrices in front of and after the isotropic Faraday element. With a lightning duration from units to tens of microseconds, we can confidently assume that the characteristics of fibre spans before (Mueller matrix $M_{\rm A}$) and after (Mueller matrix $M_{\rm B}$) a Faraday element [Mueller matrix $M_{\rm F}(t)$] are time independent:

$$M(t) = M_{\rm B} M_{\rm F}(t) M_{\rm A},$$
$$\hat{s}_{\rm out}(t) = M(t)\hat{s}_{\rm in}. \qquad (8)$$

In this case, the Mueller matrix of the isotropic Faraday element coincides with the matrix of rotation of the Poincaré sphere around the s_3 axis and has the form

$$M_{\rm F}(t) = \begin{pmatrix} \cos[\varphi(t)] & -\sin[\varphi(t)] & 0 \\ \sin[\varphi(t)] & \cos[\varphi(t)] & 0 \\ 0 & 0 & 1 \end{pmatrix}, \; \varphi(t) = 2V\int B(t,z)\,{\rm d}z. \qquad (9)$$

The $\varphi(t)$ dependence was found in [3]. Reconstruction of $\varphi(t)$ from the experimentally measured dependence $\hat{s}_{\rm out}(t)$ is possible. However, the accuracy decreases if the absolute value of the vector product of the vectors $M_{\rm A}\hat{s}_{\rm in}$ and $(0,0,1)^{\rm T}$ is close to zero, and vice versa, if the absolute value of the product is large, then the $\varphi(t)$ dependence is well restored. Thus, the use of the plane angle is convenient for describing the temporal dynamics of a Faraday element, the linear anisotropy of which can be neglected.

Similarly to the definition of the spherical polarisation rotation speed (4), we define the plane polarisation rotation speed $\Omega_{\rm p}$ as the absolute value of the time derivative of the plane angle:

$$\Omega_{\rm p}(t) = \left|\frac{{\rm d}\varphi}{{\rm d}t}\right|. \qquad (10)$$

4. Lightning strike-induced Faraday effect

As shown in [4], during a lightning strike, an electric current i is induced in the ground wire, the directions of which are opposite to the left and right of the point of the lightning strike, and the current value at point z is described by the function of the current shape I with a time delay equal to the transit time of the electromagnetic wave between a point of the lightning strike and a point with coordinate z (Fig. 1):

$$i(t,z) = \frac{1}{2}I(t - |z|/c)\,{\rm sign}(z), \qquad (11)$$

where c is the speed of light.

For further calculations, it is convenient to use a coordinate system in which the origin of coordinates is located at a point where lightning strikes the ground wire. We will assume that the light wave propagates from left to right (Fig. 1). Let us designate the left coordinate as $z = -L_1$, and the right one as $z = L_2$, with $L_1 + L_2 = L$ being the distance between the pylons.

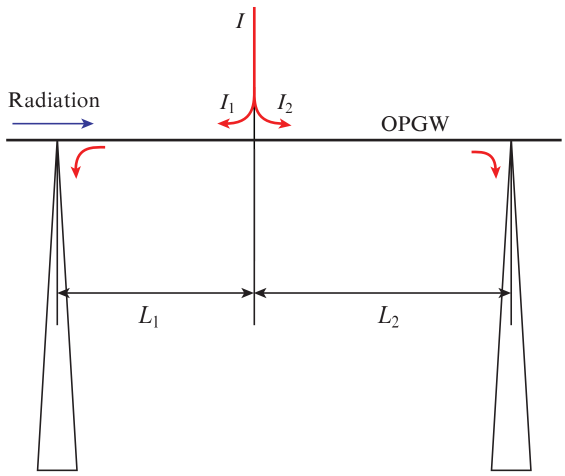

Figure 1. Schematic of lightning strike and current spreading.

The rotation of the polarisation state of the light signal under the action of the lightning-induced magnetic field occurs in the region from $z = -L_1$ to $z = L_2$. We assume that at the moment of time t_0 the optical signal in fibre passes through point $z = 0$ (Fig. 2). Then the magnitude of the circular birefringence induced by the magnetic field due to the Faraday effect in the span dz with the coordinate z for the light wave passing through the origin (point of lightning strike) at the time moment t_0 is determined by the expression

$${\rm d}\varphi = 2VB(t,z)\,{\rm d}z, \qquad (12)$$

where $t = t_0 + nz/c$ is the relationship between the time t_0, when the light wave crosses the origin of coordinates, and the time t, when the same light wave crosses the point z (Fig. 2); and n is the refractive index of optical fibre. The electric current flowing through the optical ground wire, due to the twisting of the conductive wires, forms a longitudinal magnetic field inside the ground wire, which is determined by the formula

$$B(t,z) = \frac{\mu_0}{d} i(t,z), \tag{13}$$

where μ_0 is the vacuum permeability (it is taken equal to $4\pi \cdot 10^{-7}$ H m^{-1}); and d is the twist pitch (it is taken equal to 0.5 m in our calculations). Without loss of generality, we assume that $B(t,z)$ has a positive sign to the right of zero ($z > 0$). Taking into account (11) and (13), the differential increment of angle (12) takes the form

$$d\varphi = \frac{\mu_0 V}{d} I\left(t - \frac{|z|}{c}\right)\mathrm{sign}(z)dz$$

$$= \frac{\mu_0 V}{d} I\left(t_0 + \frac{nz}{c} - \frac{|z|}{c}\right)\mathrm{sign}(z)dz. \tag{14}$$

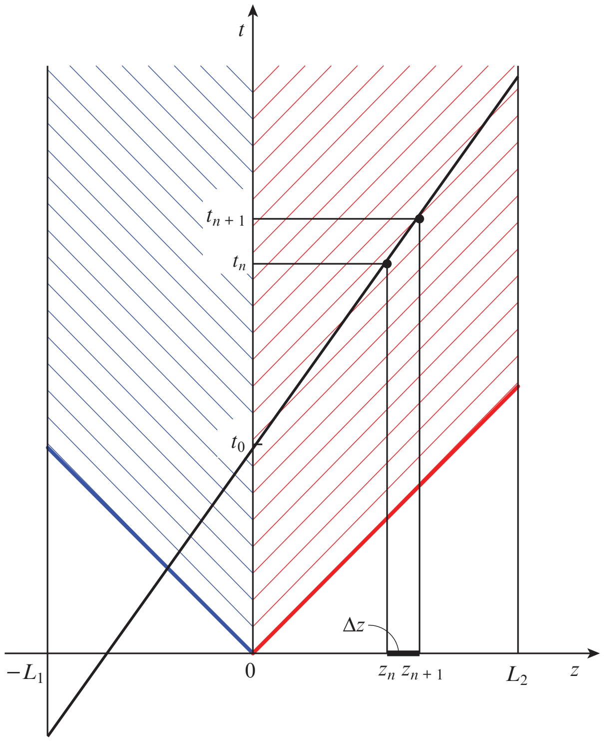

Figure 2. Minkowski space.

The sign(z) function takes into account different directions of the magnetic field to the left and to the right of the point where the lightning strikes the ground wire.

5. Results of numerical simulation of the polarisation rotation speed time profiles during a lightning strike

For numerical simulation, as in [3], we use the lightning discharge model described by a linear growth function:

$$I(t) = \begin{cases} 0, & t \leqslant 0, \\ I_{max} t/\tau, & 0 < t < \tau, \\ I_{max}, & t \geqslant \tau, \end{cases} \tag{15}$$

where τ is a constant characterising the rise time of the current pulse. This function does not take into account a slow decrease in the current, which, as a rule, is not critical, since the most significant parameter is the slope (derivative of the current with respect to time) in the section of the lightning current growth. In the calculations, τ was equal to 1 μs.

The numerical model, described in detail in the Appendix, allows one to calculate the angles describing the change in the polarisation state:

1. The spherical angle θ and the associated spherical polarisation rotation speed are most easily calculated from the dependences $s_1(t)$, $s_2(t)$ and $s_3(t)$ measured with a standard polarimeter. However, the value of this angle in the isotropic case substantially depends on the polarisation state of light, which makes it difficult to reconstruct the lightning parameters from the time dependence of the spherical angle.

2. The plane angle φ is convenient to use when analysing the Faraday effect in an isotropic region (or at a very low birefringence), since in this case it can be assumed that, upon a lightning strike, a point describing the polarisation states (measured by a polarimeter) moves along the Poincaré sphere along a circle around the s_3 axis. One can estimate the parameters of this circle, and then calculate the time dependence of the plane angle. In the isotropic case, the value of φ is directly proportional to the magnetic field in accordance with formula (9).

5.1. Anisotropic fibre

Figure 3 shows the results of numerical simulation of the polarisation rotation speed time profiles [$\Omega_p(t) = |d\varphi/dt|$ for anisotropic fibre] with a correlation length L_c = 100 m for different beat lengths L_b and different points where lightning strikes. A linear increase in the current up to I_{max} = 150 kA is considered, the distance between the pylons being L = 300 m. In the calculations, in each case, averaging is performed over 1000 realisations. The vertical lines in the curves represent the standard deviations from the mean (solid curves).

The presented polarisation rotation speed time profiles show a significant effect of fibre anisotropy characterised by the beat length L_b on the shape of the polarisation rotation speed time profile and the maximum value of the rotation speed. An increase in linear anisotropy (a decrease in the beat length) leads to a decrease in the polarisation rotation speed. The shapes of the polarisation rotation speed time profiles for beat lengths of 10, 20, and 75 m differ markedly from the isotropic case (dashed curves in Fig. 3). With an increase in the beat length (300 m), the shapes of polarisation rotation speed time profiles become more and more similar to the shapes of similar profiles in the isotropic case. Note that the polarisation rotation speed time profiles for isotropic fibre and weakly anisotropic fibre with a beat length of more than 1 km coincide with an accuracy of several percent.

5.2. Mechanism of decreasing the rate of change in the polarisation state in anisotropic fibre

Thus, the presence of randomly distributed birefringence along fibre leads to a decrease in both the angles of rotation of the polarisation state (spherical and planar) and the rate of their change in time due to the Faraday effect. Previously, it was found in [7–9] that the presence of a fixed value of bire-

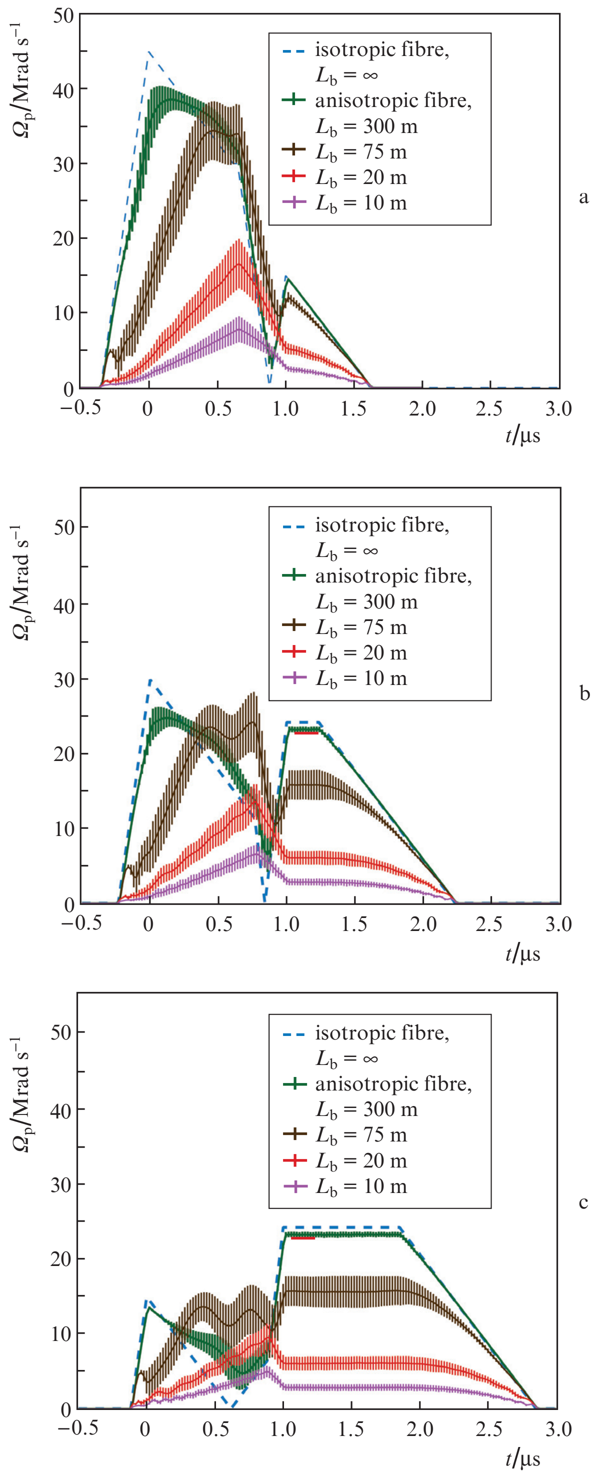

Figure 3. (Colour online) Influence of optical fibre anisotropy on the plane polarisation rotation speed time profiles $\Omega_p(t)$ for different beat lengths L_b. Dashed curves show data of analytical calculation of the absolute value of the plane palarisation rotation speed for the isotropic case ($L_b = \infty$). Coordinates of the lightning strike point are as follows: (a) $L_1 = -75$ m, $L_2 = 225$ m; (b) $L_1 = -150$ m, $L_2 = 150$ m; and (c) $L_1 = -225$ m, $L_2 = 75$ m.

fringence leads to a weakening of the Faraday effect. This can be qualitatively explained as follows. The change in polarisation during the propagation of light through a span of length L is described by the rotation of the polarisation state around an axis, the orientation of which is determined by the ratio between the values of linear and circular anisotropy, and the angle of rotation is calculated by the formula

$$\varphi(t) = \sqrt{\psi^2 + [2VB(t)L]^2}, \tag{16}$$

where $\psi = 2\pi L/L_b$ is the difference between the phase incursion. Since the magnitude of the linear anisotropy does not depend on the magnetic field, the change in the plane angle of rotation caused by the change in the magnetic field from $B = 0$ to $B(t)$ is determined by the expression

$$\varphi(B(t)) - \varphi(B = 0) = \sqrt{\psi^2 + [2VB(t)L]^2} - \psi, \tag{17}$$

the value of which is less than the angle of rotation in the isotropic case ($\psi = 0$), equal to $2VB(t)L$. With a random birefringence distribution along fibre, the picture of the motion of the point describing the polarisation state along the Poincaré sphere becomes more complicated, but the physical mechanism of decreasing the plane angle at each small span of fibre remains the same as in the case of fibre with a fixed value of linear anisotropy.

The numerical results obtained in this work show that in order to reconstruct the lightning parameters from the experimentally measured polarisation rotation speed time profiles, it is necessary to take into account anisotropy of optical fibre, which our numerical model of fibre with a random distribution of anisotropy in a magnetic field makes possible.

6. Conclusions

In this paper, the delayed field model, which was previously used to calculate the polarisation rotation speed in isotropic fibre during a direct lightning strike in an OPGW [3], is generalised to the case of anisotropic optical fibres with a random distribution of birefringence. It is shown that anisotropy of real telecommunication fibres has a noticeable effect on the shape of the polarisation rotation speed time profile and should be taken into account in analysing the effect of lightning strikes on the operation of coherent communication systems.

The numerical model of the Faraday effect in a telecommunication fibre presented in this work makes it possible to calculate the dynamics of the polarisation state upon a direct lightning strike and to calculate the time dependences of spherical and plane angles, as well as the polarisation rotation speeds.

As in the isotropic case, the shapes of the curves describing the polarisation rotation speed time profiles change when the direction of propagation of the light wave becomes opposite (except for the lightning strike exactly in the middle of the OPGW span between the pylons). Physically, this can be explained by the fact that the interaction of a travelling light signal with a short current pulse propagating in the same direction is more effective than the interaction of a light signal travelling along the OPGW with a current pulse travelling towards it.

The practical significance of this work lies in the construction of a numerical model for calculating rapid changes in the polarisation state of a light signal, which can potentially be used to calculate the parameters of a lightning strike into a ground wire. The development of a device for continuous monitoring of lightning strikes in OPGWs by measuring the polarisation state with a polarimeter will make it possible to determine the places of possible damage to the ground wire due to lightning strikes and to carry out the necessary preventive work.

It also follows from the results of the work that the destructive effect of lightning strikes on the operation of a FOCL can be weakened by using optical fibres with high linear anisotropy (short beat length L_b). However, the use of such fibres degrades the operation of FOCLs due to an increase in polarisation mode dispersion, which makes their practical use impractical. To eliminate communication interruption in the event of a lightning strike, it is advisable to use special designs of an optical ground wire and special algorithms for digital signal processing in a coherent receiver [10].

Appendix. Simulation of the Faraday effect in anisotropic fibre upon a lightning strike

In the general case, there are no analytical formulae for calculating the Faraday effect in randomly anisotropic fibre. Therefore, the calculations were carried out numerically using the generalisation (of the model proposed in [4] and having an analytical solution for isotropic fibre) to fibre with random anisotropy. In the generalised model, a fibre of length L is divided into M spans of equal length $\Delta z = L/M$. We represent the Jones matrix of each span as a product of two Jones matrices, the first of which describes weak linear birefringence caused by imperfect cylindrical fibre profile, mechanical stresses, bends, etc., and the second, weak circular birefringence induced by an external magnetic field due to the Faraday effect. Then the Jones matrix of the mth span ($m = 1, 2, \ldots, M$) will have the form $J_m = F_m G_m$, where the G_m matrix describes the weak internal linear birefringence possessed by fibre, and the F_m matrix describes the circular birefringence due to the Faraday effect (Fig. 1A). The order of the product of the almost diagonal matrices F_m and G_m for the formation of the Jones matrix of the span is not so important; the commutator of the matrices F_m and G_m defined below [see formulae (A2) and (A6)] has a quadratic order of smallness: $[F_m, G_m] = F_m G_m - G_m F_m \propto \Delta z^2$.

To calculate the Jones matrix of the entire span, we use the product of the Jones matrices of small spans Δz. We need to take into account the lag of the current and the field of the light wave, as was done in [3] for the isotropic case. Only now, instead of adding small increments of plane angles and then integrating, multiplication of the matrices responsible for birefringence and the Faraday effect should be performed. The resulting Jones matrix has the form

$$J(t_0, N) = J_M J_{M-1} \ldots J_2 J_1$$

$$= F_M G_M F_{M-1} G_{M-1} \ldots F_m G_m \ldots F_1 G_1 . \quad \text{(A1)}$$

Here

$$G_m = R_m G R_m^{-1} \quad \text{(A2)}$$

is the Jones matrix of the birefringent plate rotated by a random angle around the z axis;

$$R_m = \begin{pmatrix} \cos\alpha_m & \sin\alpha_m \\ -\sin\alpha_m & \cos\alpha_m \end{pmatrix}$$

are the matrices of rotation through the angle α_m; and

$$G = \begin{pmatrix} \exp(i\psi/2) & 0 \\ 0 & \exp(-i\psi/2) \end{pmatrix}$$

is the matrix of a birefringent element. The difference between the phase incursions ψ is determined by the beat length according to the formula $\psi = 2\pi\Delta z/L_b$.

The random distribution of orientations of the main axes of the spans in the model will be described by a random process with a white noise spectrum [11]. Each span of fibre is twisted relative to the previous one around the z axis by a random angle $\Delta\alpha_m$ obeying a normal distribution with variance σ and zero mean. The dependence of the probability density on the angle $\Delta\alpha_m$ is expressed as:

$$f(\Delta\alpha_m) = \frac{1}{\sqrt{2\pi}\sigma} \exp\left(-\frac{\Delta\alpha_m^2}{2\sigma^2}\right). \quad \text{(A3)}$$

Thus, one random realisation is formed $(\Delta\alpha_1, \Delta\alpha_2, \ldots, \Delta\alpha_M)$. The angles of orientations of the axes of the spans are related to the relative angles of rotation of the spans by the expression

$$\alpha_m = \sum_{i=1}^{m} \Delta\alpha_i, \;\; m = 1, 2, \ldots, M. \quad \text{(A4)}$$

The squared variance is proportional to the span length and inversely proportional to the correlation length L_c:

$$\sigma^2 = \frac{\Delta z}{2L_c}. \quad \text{(A5)}$$

Let us define the matrices F_m ($m = 1, \ldots, M$), included in expression (A1). In the presence of a magnetic field, in the Cartesian basis the matrices F_m describing the circular birefringence induced by the magnetic field due to the Faraday effect have the form

$$F_m = \begin{pmatrix} \cos(\Delta\varphi_m/2) & -\sin(\Delta\varphi_m/2) \\ \sin(\Delta\varphi_m/2) & \cos(\Delta\varphi_m/2) \end{pmatrix}. \quad \text{(A6)}$$

Passing from the differential increment of the phase difference $d\varphi_m$ of left and right circular polarisations [see formula

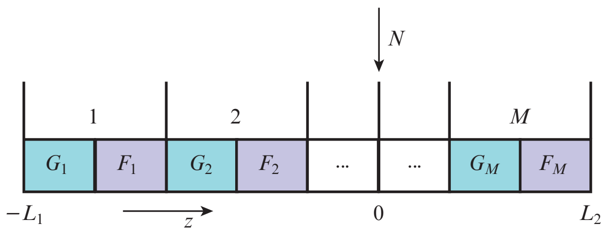

Figure 1A. Splitting of fibre by physical processes into alternating subspans with matrices G_m and F_m describing linear and circular birefringence. Lightning strikes the point between the spans. It is convenient to set this point by a half-integer number N, so that to the left of it there is a span with the number $N - 1/2$, and on the right, with the number $N + 1/2$.

(14)] to a small increment $\Delta\varphi_m$ related to the mth span, we obtain the expression

$$\Delta\varphi_m(N,t_0) = \frac{\mu_0 V}{d} I$$

$$\times\left(t_0 + \frac{nz_m(N)}{c} - \frac{|z_m(N)|}{c}\right)\text{sign}[z_m(N)]\Delta z, \qquad \text{(A7)}$$

where $z_m(N) = (m - N)\Delta z$; $m = 1,2,\ldots,M$; and $N = 1/2, 1 + 1/2,\ldots,$. At $N = 1/2$, the point of lightning strike is close to the left pylon, and at $N = M + 1/2$, to the right onew. Relationship (A7) takes into account the dependence of $\Delta\varphi_m$ on the point of impact of lightning (N) and on the moment of time t_0, when the signal from the mth span crosses the origin of coordinates, i.e. the point of impact of lightning. The resulting Jones matrix $J(t_0, N)$ describes the dynamics of the polarisation properties of the fibre span between the pylons of length $L = M\Delta z$ at $L_1 = (N - 1/2)\Delta z$, $L_2 = (M - N + 1/2)\Delta z$.

We assume that the time t_0 runs through the discrete values $t_1 = t_{\min}, t_2,\ldots, t_k = t_{\max}$, experiencing the same increments of Δt. Consider the resulting Jones matrix (A1) at successive times t_{k-1} and t_k ($k > 1$). Introducing the matrix ΔJ_k of the transition from the state at the moment of time t_{k-1} to the state at the moment of time t_k, we write the formal equality

$$J(t_k) = \Delta J_k J(t_{k-1}). \qquad \text{(A8)}$$

Thus we obtain

$$\Delta J_k = J(t_k)J^{-1}(t_{k-1}) = J(t_k)J^{+}(t_{k-1}). \qquad \text{(A9)}$$

The Jones matrix ΔJ_k corresponds to rotation in the Stokes space by an angle $\Delta\beta_k$ around the unit vector $\hat{\boldsymbol{b}}_k$. The components of the vectors $\hat{\boldsymbol{b}}_k = (b_{1k}, b_{2k}, b_{3k})^{\mathrm{T}}$ and the angles $\Delta\beta_k$ are related to the matrix ΔJ_k by the expression [12]

$$\Delta J_k = E\cos(\Delta\beta_k/2)$$

$$- \mathrm{i}(b_{1k}\sigma_1 + b_{2k}\sigma_2 + b_{3k}\sigma_3)\sin(\Delta\beta_k/2), \qquad \text{(A10)}$$

where E is the identity matrix; and

$$\sigma_1 = \begin{pmatrix} 1 & 0 \\ 0 & -1 \end{pmatrix}, \quad \sigma_2 = \begin{pmatrix} 0 & 1 \\ 1 & 0 \end{pmatrix}, \quad \sigma_3 = \begin{pmatrix} 0 & -\mathrm{i} \\ \mathrm{i} & 0 \end{pmatrix} \qquad \text{(A11)}$$

are the Pauli matrices used in polarising optics. In fact, the Mueller matrix ΔM_k corresponding to the Jones matrix ΔJ_k rotates the Poincaré sphere through the angle $\Delta\beta_k$ around the unit vector $\hat{\boldsymbol{b}}_k$. The quantities $\Delta\beta_k$ and $\hat{\boldsymbol{b}}_k$ are determined by the formulae [12]

$$\cos\left(\frac{\Delta\beta_k}{2}\right) = \frac{1}{2}\mathrm{Tr}(\Delta J_k),$$

$$b_{ik}\sin\left(\frac{\Delta\beta_k}{2}\right) = \frac{\mathrm{i}}{2}\mathrm{Tr}(\sigma_i \Delta J_k), \; i = 1,2,3, \qquad \text{(A12)}$$

or, taking into account the smallness of the angles $\Delta\beta_k$, according to the formulae

$$\Delta\beta_k = 2\arccos\left[\frac{1}{2}\mathrm{Tr}(\Delta J_k)\right],$$

$$b_{ik} = \frac{\mathrm{i}}{2}\frac{\mathrm{Tr}(\sigma_i \Delta J_k)}{\sin(\Delta\beta_k/2)}, \quad i = 1,2,3. \qquad \text{(A13)}$$

The result obtained can be interpreted as follows: the output state of polarisation in the Stokes space moves along the Poincaré sphere, performing successive rotations, so that the rotation in the time interval (t_{k-1}, t_k) occurs around the unit vector $\hat{\boldsymbol{b}}_k$ by the angle $\Delta\beta_k$. Small angles $\Delta\beta_k$ are equal to small plane angles $\Delta\varphi_k$.

References

1. Verdet E. *Recherches sur les Propriétés Optiques Développées dans les Corps Transparents par L'action du Magnétisme* (Paris: Mallet-Bachelier, 1863).
2. Charlton D. *Opt. Express*, **25** (9), 9689 (2017).
3. Konyshev V.A. *Laser Phys. Lett.*, **18** (11), 115101 (2021).
4. Konyshev V.A. *Quantum Electron.*, **49** (8), 773 (2019) [*Kvantovaya Elektron.*, **49** (8), 773 (2019)].
5. Mansuripur M. *Opt. Photonics News*, **10** (11), 32 (1999).
6. Cruz J., Andres M., Hernandez M. *Appl. Opt.*, **35** (6), 922 (1996).
7. Harms H., Papp A., Kempter K. *Appl. Opt.*, **15** (3), 799 (1976).
8. Smith A.M. *Appl. Opt.*, **17** (1), 52 (1978).
9. Stolen R., Turner E. *Appl. Opt.*, **19** (6), 842 (1980).
10. Akopov S., Konyshev V., Nanii O., Treshchikov V., Ubaydullaev R., Frolov I. *Last Mile*, **4** (96), 24 (2021) [*Pervaya Milya*, **4** (96), 24 (2021)].
11. Wai P., Menyuk C. *Opt. Lett.*, **19** (19), 1517 (1994).
12. Gordon J., Kogelnik H. *Proc. Nat. Acad. Sci. USA*, **97** (9), 4541 (2000).